applied sciences

MDPI

Article

A Compact Accelerator-Based Light Source for High-Power, Full-Bandwidth Tunable Coherent THz Generation

Kaiqing Zhang [1], Yin Kang [2,3], Tao Liu [1], Zhen Wang [1], Chao Feng [1,*], Wencheng Fang [1] and Zhentang Zhao [1]

[1] Accelerator Physics and Laser Technology Department, Shanghai Advanced Research Institution, Chinese Academy of Sciences, Shanghai 201210, China; zhangkaiqing@zjlab.org.cn (K.Z.); liutao@zjlab.org.cn (T.L.); wangzhen@zjlab.org.cn (Z.W.); fangwencheng@zjlab.org.cn (W.F.); zhaozhentang@zjlab.org.cn (Z.Z.)
[2] University of Chinese Academy of Sciences, Beijing 100049, China; kangyin@sinap.ac.cn
[3] Accelerator Physics and Laser Technology Department, Shanghai Institute of Applied Physics, Chinese Academy of Sciences, Shanghai 201800, China
* Correspondence: fengchao@zjlab.org.cn

Featured Application: This work can be used to generate coherent THz radiation with tunable frequency and pulse energy to satisfy various requirements of different scientific frontiers, such as THz pump-probe, THz triggered chemistry, and single-shot THz bioimaging.

Abstract: Terahertz (THz) radiation sources are increasingly significant for many scientific frontiers, while the generation of THz radiation with high-power at wide-tunable frequencies is still a limitation for most existing methods. In this paper, a compact accelerator-based light source is proposed to produce coherent THz radiation with high pulse energy and tunable frequency from 0.1 THz to 60 THz. By using a frequency beating laser-modulated electron beam and undulator taper, intense coherent THz radiation can be generated through undulators. Theoretical analysis and numerical simulations demonstrate that the proposed technique can generate narrow-bandwidth THz radiation with a pulse energy up to 6.3 millijoule (mJ) and the three-dimensional effects of beam has limited influence on its performance. The proposed technique will open up new opportunities for THz spectroscopic and time-resolved experiments.

Keywords: coherent THz; frequency beating; wide-tunable THz frequency; free electron laser

Citation: Zhang, K.; Kang, Y.; Liu, T.; Wang, Z.; Feng, C.; Fang, W.; Zhao, Z. A Compact Accelerator-Based Light Source for High-Power, Full-Bandwidth Tunable Coherent THz Generation. *Appl. Sci.* **2021**, *11*, 11850. https://doi.org/10.3390/app112411850

Academic Editor: Sanathana Konugolu Venkata Sekar

Received: 28 October 2021
Accepted: 12 December 2021
Published: 13 December 2021

1. Introduction

Terahertz (THz) radiation contributes to many scientific frontiers by serving as a nonionizing probe in nonlinear optics, pump experiments, spectroscopic, and time-resolved applications [1–3]. In the last decades, there has been significant interests in the generation of terahertz (THz) radiation with superior properties, for instance, ultra-high pulse energy, tunable wavelength at full THz frequency range, and full temporal coherence. Many fantastic scientific applications such as THz-assisted high-order harmonic generation, THz-triggered chemistry, and single-shot THz bioimaging require THz radiation with pulse energy up to millijoule (mJ) level [4–6], which remains a challenge for most THz generation methods. Furthermore, generating THz radiation with mJ level pulse energy at full THz frequency range can be even more difficult for the existing THz techniques.

Currently, the prominent methods to generate high-power THz pulses are generally based on the ultrafast laser techniques [7–11], laser-produced plasmas techniques [12–17], or electron accelerator-based methods. The ultrafast laser technique, called optical rectification and optical parametric amplifier, has been employed to generate THz pulses with a maximum pulse energy of about 900 μJ from organic crystals [9], while it has limitations on further increases in the peak power and repetition rate due to the low inherent optical damage threshold of crystals [11]. The laser-produced plasma technique is generally immune

to the damage threshold since a damage-free medium is utilized to achieve an intense THz pulse. Laser-driven gas-density plasma can generate THz radiation with a pulse energy of a few mJ level, then saturation happens with the increasing of the energy of the pump laser [13,14]. By contrast, laser-solid interaction can achieve THz radiation with a pulse energy of several hundreds of mJ but the spectral coverage is quite limited [15,16]. Recently, coherent THz radiation with exceeding multi-millijoules is demonstrated by utilizing an ultra-intense, picosecond (ps) laser pulse to irradiate a metal foil, while it can only produce THz radiation at relative low frequency (lower than 3 THz) [17].

The electron accelerators have reliable abilities to produce THz radiation via several different ways: coherent synchrotron radiation (CSR) [18–21], optical transition radiation (OTR), coherent optical transition radiation (COTR) [22–25], or undulator radiation [26–28]. The CSR radiation at the THz range can be simply generated from a magnetic dipole in the storage ring [18,19]. Generation of tunable coherent THz radiation with a pre-bunched electron beam has also been demonstrated in the storage ring, but with a relatively low power and long pulse length [20]. The CSR radiation can also be achieved with the linac accelerator where one single pass radiation will limit the radiation at low gain level and the output bandwidth is quite broad [21]. The OTR emits when the relativistic electron beam crosses the boundary of two different medias, which can generate the radiation from X-ray to microwaves, while the radiation generally has a broadband spectrum and a maximum pulse energy of hundreds μJ (350 μJ [24] and 140 μJ [25]). In addition, a special Smith–Purcell radiation from cylindrical grating is applied to obtain coherent THz radiation below 1 THz with a pulse energy of 0.8 μJ from high harmonics [29].

Free electron laser (FEL) [30–32] is recognized as a new generation light source, which has the capability of providing ultra-short pulses with gigawatt (GW) level peak power and tunable wavelength from THz to hard X-ray. Most of the FEL facilities adopt afterburners to generate intense THz radiation by using a compressed electron bunch with the duration shorter than one THz period; therefore, no high gain process is expected and the radiation power is usually limited to a maximal pulse energy of hundreds μJ (200 μJ [21] and 100 μJ [33]). Powerful narrow-band THz pulses can be produced by using a sub-picosecond (ps) scale pulse train, which can be generated either by directly illuminating the photocathode with a train of laser pulses [34–36] or manipulating the electron beam at relativistic energy (including exchanging transverse modulation to longitudinal distribution [37,38], direct modulating the drive laser [39], converting wakefield induced energy modulation to density bunching [40], two wavelengths of energy modulation in two separated undulator sections [41,42], slice energy spread modulation [43], and laser-based density modulation [44,45]). Comparing with the former method with the laser pulse train, the electron beam manipulation method has the advantage of more flexible tunability in the output frequency and can exclude the negative effects from the space charge force, which may smear out the longitudinal structures at low beam energy. Previously, simulation studies on THz FEL using a laser modulator and a bunch compressor have been performed, which use an assumed THz seed laser [45].

In this paper, a dedicated compact light source based on electron beam manipulation is proposed for generating mJ-level high energy radiation pulses with a tunable frequency from 0.1 THz to 60 THz. In this proposal, the pulse shaping and chirped frequency beating techniques [20,46] are utilized, and two cogenetic chirped laser pulses are employed to form optical heterodyning, thus obtaining the quasi-sinusoidal optical signal at THz wavelength. This optical pulse helps to form coherent bunching at THz frequency in the electron beam, which can be used for generating intense THz radiation in the following undulators. To achieve THz radiation with higher peak power and pulse energy, an electron beam with long pulse length and undulator taper are utilized to get longer interaction length and keep lasing after saturation. To achieve a radiation at full THz range, an initial ultra-fast and high-power laser is utilized to achieve a longer time delay and harmonic lasing is also used to furtherly increase upper limit of THz frequency. In this paper, the detail descriptions of the basic principle of this proposal and start-to-end simulations with realistic parameters

and three-dimensional effects are presented. This proposal can be easily realized by using a compact accelerator facility with the electron beam energy of tens of MeV and mature accelerator and laser technologies.

2. Method and Principles

Figure 1 shows the schematic layout of the proposed technique. The electron beam is produced from a photocathode gun with a beam energy of several keV, sequentially the beam energy will be enhanced to tens of MeV by a short LINAC. Then the electron beam is sent into a short undulator (modulator) to interact with a chirped frequency beating laser pulse and get sufficient energy modulation. This energy modulation is converted into density modulation by a small chicane. After that, the bunched electron beam will emit intense coherent THz radiation in the following radiator. In the proposed technique, the critical point is the preparation of the seed laser, which involves tunable THz frequency signal. This process contains the optical heterodyning of two linearly chirped broadband pulses, as presented in Figure 1. To generate the required seed laser, ultra-fast laser pulses are stretched to create large frequency chirps. Here, we consider a Gaussian optical pulse with a central frequency at ω_0, an initial amplitude of $2A$ and a transform-limited bandwidth of σ. The electrical field can be written as $E_0 = 2Ae^{-(i\omega_0 t + \frac{t^2}{\sigma^2})}$. After propagating through a linearly dispersive medium, the laser pulse undergoes a frequency-dependent phase modulation, which can be written as [46]:

$$\phi(\omega) = \phi(\omega_0) + \tau_0(\omega - \omega_0) + \frac{(\omega - \omega_0)^2}{2\mu} + \dots , \quad (1)$$

where τ_0 is the group delay at ω_0, μ is the carrier frequency sweep rate (linear chirp rate), $\mu = \frac{d\omega}{dt}$. The chirped laser pulse firstly passes through the optical pulse stretcher (generally based on gratings) to broaden the pulse length of the lasers to σ_n. when $\sigma_n \gg \sigma$, σ_n can be calculated as $\sigma_n = \sigma\sqrt{(1 + 4/\mu^2\sigma^4)}$. The optical pulse stretcher can disperse the chirped pulse to different position, thus broadening the pulse length, which can be tuned as required. Here we ignore the high-order chirps, and the electrical field of the laser pulse becomes

$$E_f = A\sqrt{\frac{\sigma}{\sigma_n}}e^{-[\frac{t^2}{\sigma_n{}^2}(1 - i\frac{\sigma_n}{\sigma})]} \times e^{i[\phi_0 - \omega_0(t+\tau_0) - \frac{\pi}{4}]}. \quad (2)$$

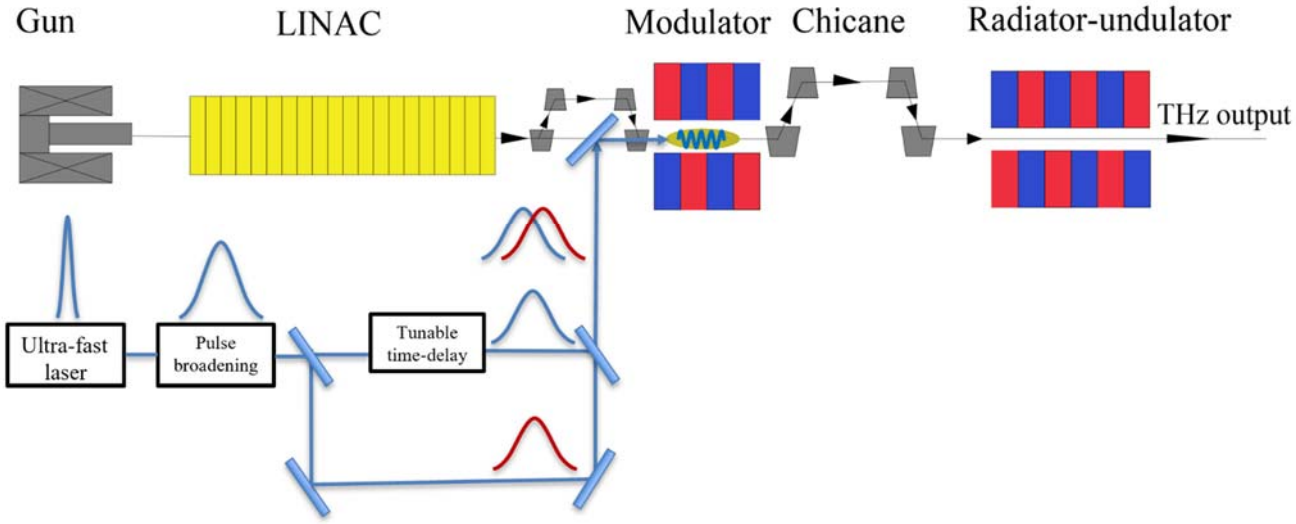

Figure 1. Schematic layout of the proposed technique. The length from photocathode gun to the exit of chicane is about 25 m (include photocathode gun, LINAC, modulator, chicane, and drifts), the total undulator length is about 10–15 m (a undulator length of 4 m is enough for FEL saturation, tapered undulators are required to obtain higher pulse energy).

After that, a beam splitter is used to split the initial ultra-short pulse and send them to two branches. One of the branches contains a delay line (for example, a Michelson interferometer arrangement) that is utilized to control the time delay τ between these two pulses. Finally, the two laser pulses are recombined and sent into the modulator. Considering that these pulses are linearly chirped, the frequency content of the two pulses at every point in time domain differs by a constant frequency f_0, which is determined by the time delay τ and initial frequency chirp. The intensity of the combined pulse is then given by

$$I = \frac{1}{2}\left|E_f\left(t+\frac{\tau}{2}\right)+E_f\left(t+\frac{\tau}{2}\right)\right|^2 = I^+(t)+I^-(t)+{E_0}^2\left(\frac{\sigma}{\sigma_n}\right)\times e^{\left(-\frac{t^2}{{\sigma_n}^2}\right)}e^{\left(-\frac{\tau^2}{2{\sigma_n}^2}\right)}\times\cos\left(\frac{2t\tau}{\sigma\sigma_n}+\omega_0\,\tau\right), \tag{3}$$

where $I^{\pm}(t) = {E_0}^2\left(\frac{\sigma}{2\sigma_n}\right)e^{-2\left(\pm\frac{\tau}{2}\right)^2/{\sigma_n}^2}$ is the intensity of low-frequency (DC) component. The last cross term is the quasi-sinusoidal term with beating frequency, which is given by:

$$f = \frac{\tau}{\pi\sigma\sigma_n} \cong \frac{\mu\tau}{2\pi}. \tag{4}$$

According to Equation (4), one can clearly find the beating frequency is proportional to the time delay τ and the linear chirp rate μ; thus, it can be easily adjusted by tuning the energy chirp and the time delay of the two laser pulses.

Figure 2 shows the relation of the calculated beating frequency f (THz) (based on Equation (4) with the time delay τ and the linear chirp rate μ ($(rad/s)^2$). One can find that the up-limit of the beating frequency is determined by the product of μ and τ. As the beating wave will only occur in the intersection of these two laser pulses, τ cannot be too large to keep sufficient power for the energy modulation. As a result, the acceptable time delay of the two pulses is determined by the peak power of the initial laser pulse. Here, as an example, we consider an ultrafast Fourier-transform-limit Gaussian laser (Coherent Inc., Santa Clara, CA, USA) with pulse length of 30 fs (RMS) and peak power of 2 MW. Assuming that the laser pulse is stretched to about 300 fs (RMS), the linear chirp rate is about 8.05×10^{25} ($(rad/s)^2$) and the τ is tuned as 900 fs. According to Equation (4), the beating frequency for this case is about 11.5 THz. In the following section, we will show the simulation results of this case. To show the beating frequency limit, we also consider an ultrafast laser with pulse length of 30 fs (RMS) and higher peak power. Assuming that the laser pulse is stretched to 300 fs and the time delay is $\tau = 2.3$ ps, the beating frequency for this case is about 30 THz. The required peak power of the initial laser pulse can be calculated by

$$P_0 \;\approx\; 2\times10^4\;P_b\sigma_n/\sigma. \tag{5}$$

As we will show below, the required minimum power of the combined pulse for energy modulation P_b is about 10 kW, so P_0 can be calculated as 2 GW, which can be easily achieved for a commercial ultrafast laser (Coherent Inc., Santa Clara, CA, USA). At the same time, the beating frequency at 0.1 THz can be easily achieved with a time delay of 0.3 ps and a frequency linear chirp rate of 1.75×10^{24} $(rad/s)^2$. Therefore, this method can generate optical signal at THz frequency from 0.1 THz to 30 THz by simply adjusting the linear chirp rate and the time delay of laser pulses. If one wants to generate higher frequency, initial laser with shorter pulse length or relative larger time delay is required.

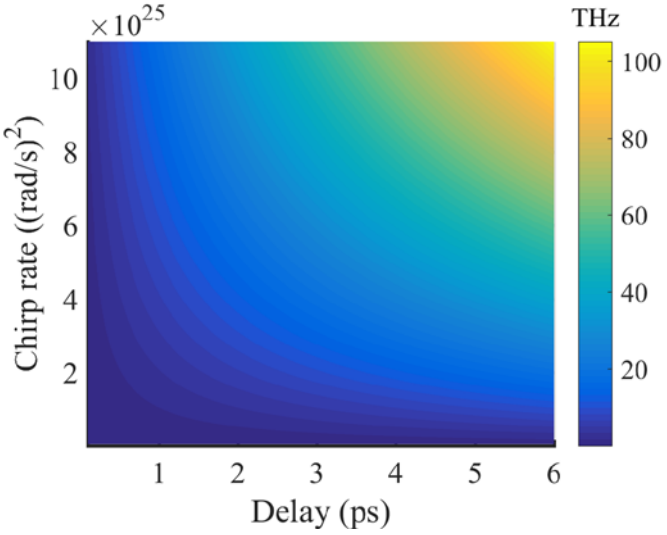

Figure 2. The relation of the calculated beating frequency f (THz) (based on Equation (4) with the time delay τ (ps) and the linear chirp rate μ $((\mathrm{rad/s})^2)$.

The combined laser pulse serves as a seed laser to modulate the electron beam. Assuming an initial Gaussian beam distribution with the average energy E_0, the dimensionless energy deviation of a particle $p = (E - E_0)/\sigma_E$, σ_E is the energy spread, and E is the beam energy. Following the Ref. [47], the initial longitudinal phase space distribution can be written as

$$f_0(p) = N_0(2\pi)^{-1/2}e^{-p^2/2}, \tag{6}$$

where N_0 is the number of electrons per unit length of the beam. The modulator resonates at the wavelength of the seed laser. The frequency beating pulse interacts with the electron beam in the modulator, where numerous fine structures appear in the longitudinal phase space of electron beam. The dimensionless energy deviation p_1 become

$$p_1 = p + Asin(\omega z/c), \tag{7}$$

where ω is the frequency of seed laser. A is the energy modulation amplitude normalized to the initial energy spread of electron beam, which can be calculated by

$$A = k_L K L_u [JJ]_1 \sqrt{\frac{Z_0 P_L}{\pi k_L Z_R (mc^2/e)^2}}/\gamma, \tag{8}$$

where k_L is the wave number of the seed laser, K is the modulator dimensionless parameter, L_u is the period of undulator, $[JJ]_1$ is the polarization modification factor for a linearly polarization planar undulator, $Z_0 = 377\ \Omega$ is the vacuum impendence, P_L is the laser power, Z_R is the Rayleigh length of the seed laser, and γ is the relative beam energy. After the energy modulation, the electron beam passes through a magnetic chicane with the dispersion strength R_{56} to convert the energy modulation into density modulation, and the longitudinal position of electron becomes

$$z_1 = z + R_{56} p \sigma_E / E_0, \tag{9}$$

The magnetic strength of chicane is required to be optimized to obtain sufficient large bunching factors at fundamental and high harmonics of the beating frequency.

Here, we consider a typical high gain FEL to generate THz radiation using the bunched electron beam, the pre-bunched electron beam ($\lambda = c/f$) is sent into an undulator, which is resonant at the fundamental or high harmonics of the beating frequency. The electron beam will initiate coherent radiation and amplify it to saturation when passing through

the undulator. Using a combined pulse with a beating frequency of 30 THz, radiation with a frequency of 30 THz and 60 THz can be generated by amplifying the bunching signals at fundamental and second harmonic of beating frequency respectively. To cover the frequency range from 0.1 to 60 THz, the electron beam energy needs to be changed and variable gap radiators with different periods are required.

3. Results

3.1. Generation of Frequency Beating Laser Pulse

To illustrate the feasibility of the proposed technique, start-to-end simulations are performed in this section. Here, we adopt a longitudinal Gaussian laser pulse at 800 nm with a duration of 30 fs and a peak power of 2 MW as the seed laser (Coherent Inc., Santa Clara, CA, USA). The laser pulse is sent into an optical pulse stretcher to stretch the pulse length to 300 fs, and the longitudinal power distribution as well as the Wigner function [48,49] are shown in Figure 3. After passing through the optical beam-splitter and Michelson interferometer, the pulse longitudinal power distributions are shown in Figure 3c, where the two laser pulses are delayed by 900 fs.

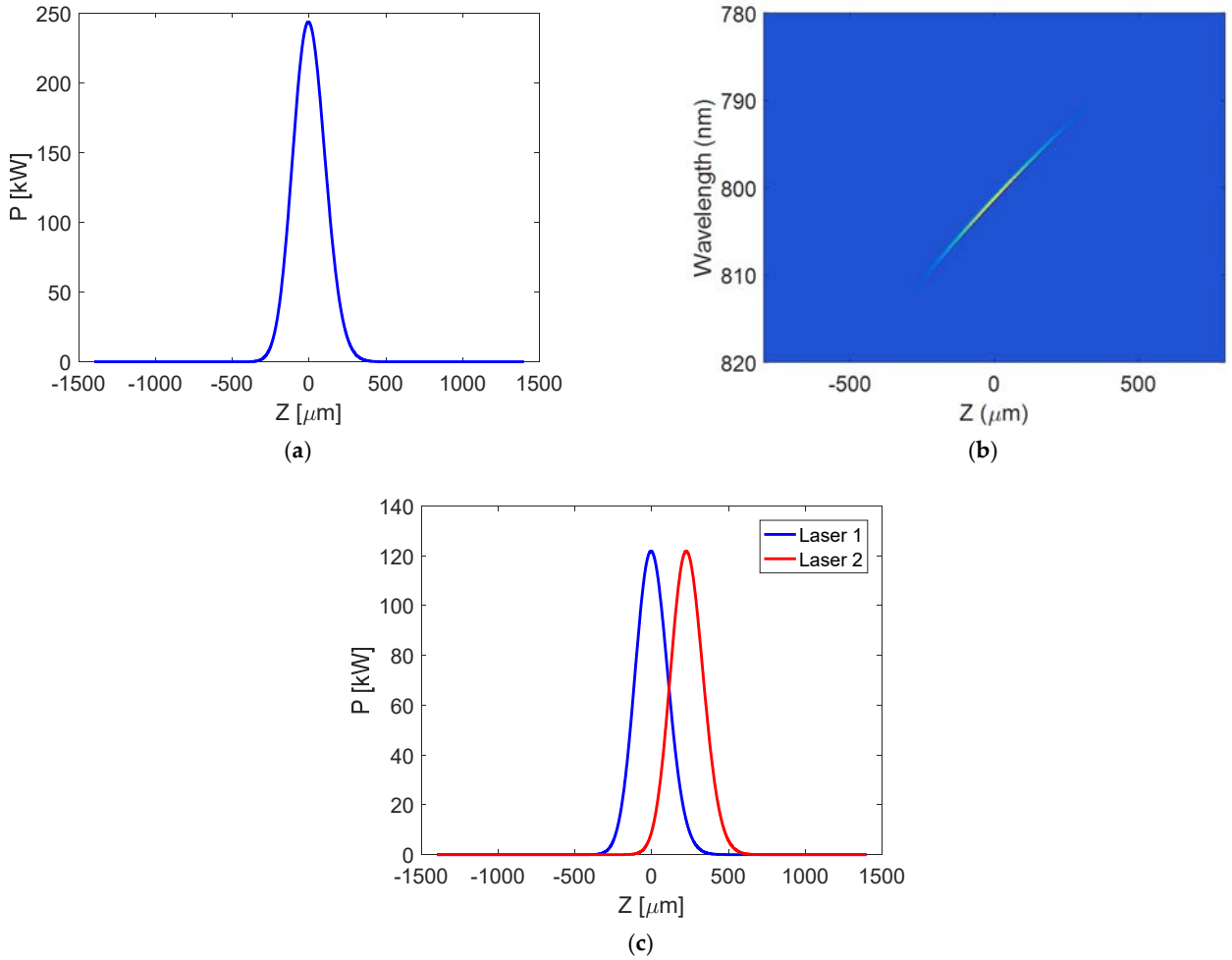

Figure 3. (**a**) The pulse longitudinal distribution after the optical pulse stretcher; (**b**) The Wigner function after the optical pulse stretcher; (**c**) the pulse longitudinal power distributions after the optical beam-splitter and Michelson interferometer.

Using the optical combiner, the two seed lasers are sequentially combined as one laser pulse, whose square root of power distribution and field amplitude are presented in Figure 4, where one can observe the wave packets at THz wavelength in the longitudinal amplitude distribution, indicating that optical signal at THz frequency has been generated. To obtain the exact value of beating frequency, Fourier-transform at time-frequency domain

is carried out and the results are also presented in Figure 4, where the fundamental frequency is about 11.5 THz.

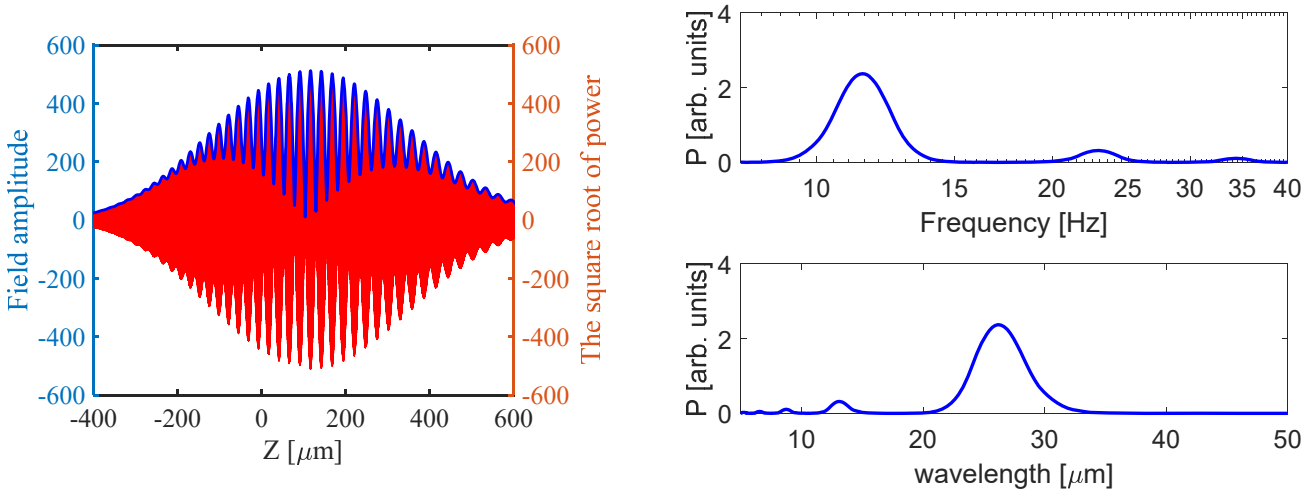

(**a**) (**b**)

Figure 4. (**a**) The square root of power distribution and field amplitude of the combined laser pulse; (**b**) the frequency and wavelength of the frequency-beating pulse.

3.2. Performance of the THz Radiation with Undulator at 11.5 THz and 23 THz

Start-to-end simulations are performed with ASTRA [50], FALCON [51], and GENESIS [52] using the typical parameters listed in Table 1. ASTRA is firstly used to simulate the electron beam dynamics in the photoinjector, which consists of an L-band Pitz gun and four L-band accelerating structures. A longitudinal uniform beam is generated in the gun with a charge of 4 nC and peak current of about 300 A. The electron beam is compressed by the velocity bunching process [53] to about 520 A in the first accelerating cavity and then boosted to about 54 MeV in the downstream accelerating structures. Figure 5 shows the longitudinal phase space of electron beam and the current profile at the exit of the linac. One can find that there is a quasi-linear energy chirp and quasi-Gaussian current profile along the longitudinal position.

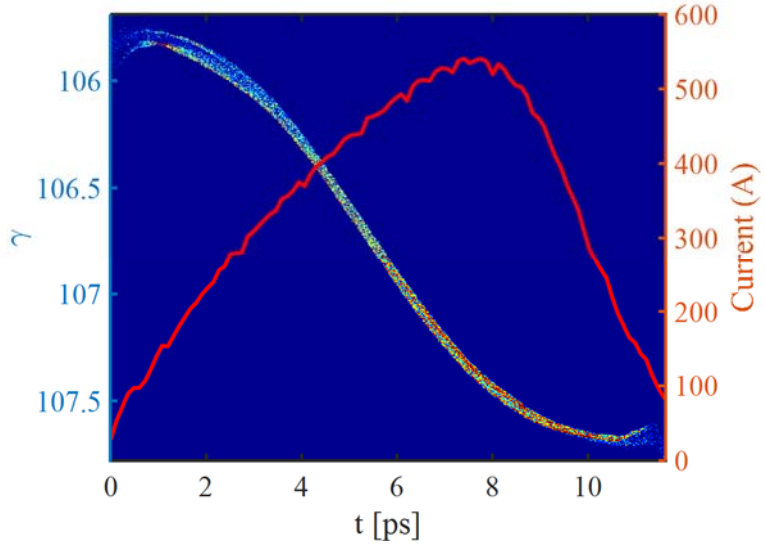

Figure 5. The longitudinal phase space of electron beam at the exit of the linac (**left**); The current profile at the exit of the linac (**right**).

Table 1. Main parameters of a THz light source.

Parameters	Value
Electron beam energy	6–70 MeV
Energy spread (slice)	0.01%
Peak current	~520 A
Bunch length	10 ps
Bunch charge	4 nC
Normalized emittance	~3.5 μm-rad
Seed laser wavelength	800 nm
THz frequency	0.1–100 THz
THz wavelength	3 μm–3 mm
Undulator period	10 cm

The electron beam and the frequency beating laser pulse are simultaneously sent into a modulator with period length of 1.6 cm and total length of 1.5 m, which is resonant at 800 nm. The modulation processes are performed with FALCON. After interacting with the frequency beating laser, the electron beam is modulated with an energy envelope at a THz wavelength (26 μm). The modulation strength is proportion to the amplitude of the laser pulse. Then the electron beam is sent through a magnetic chicane to transfer the initial energy modulation into density modulation. In Figure 6, the longitudinal phase spaces before and after the dispersion section are presented. In addition, the current profile and bunching factors at different frequencies are also given. From Figure 6b,c one can find there is apparent density modulation at THz wavelength, which results in the bunching factors at 11.5 THz (26 μm) and 23 THz (13 μm) of about 0.28 and 0.18, respectively.

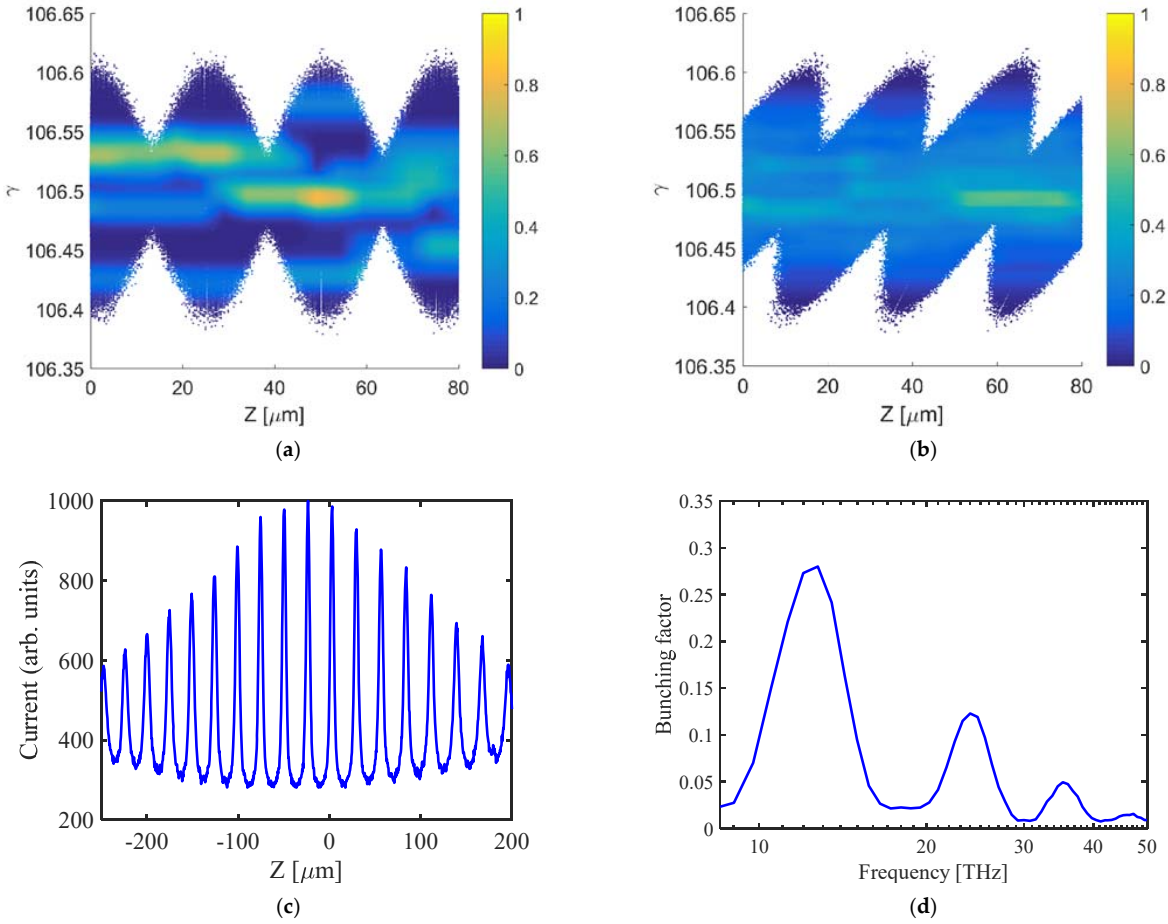

Figure 6. (**a**) The longitudinal phase space before the dispersion section; (**b**) the longitudinal phase space after the dispersion section; (**c**) the current profile after the dispersion section; (**d**) the bunching factor after the dispersion section.

To generate radiation at 11.5 THz, the bunched electron beam passes through an undulator with magnetic period of 10 cm and dimensionless parameter of 2.2. Simulations are performed with GENESIS. Figure 7 shows the peak power and bunching factor evolutions along the undulator. According to Figure 7, the power gets saturation at the undulator position of only about 3 m with a peak power of about 500 MW. Undulator taper is utilized to further enhance the radiation power. The peak power increases to about 3.2 GW at the undulator position of about 10 m. Meanwhile, the final spectrum and the power profile are also presented in Figure 7. From Figure 7, one can observe that the radiation has great longitudinal coherence with a FWHM (full width at half maximum) spectral bandwidth of about 0.05 and the final FWHM pulse length is about 400 μm (1.3 ps). The single pulse energy is about 6.3 mJ. To generate radiation at 23 THz, the bunched beam passes through the same undulator with dimensionless parameter of 1.37. The simulation results are shown in Figure 8, where the final peak power can reach about 2.3 GW at the undulator position of about 12 m and the total pulse energy of single pulse is 5 mJ. According to Figure 7, one can also observe that the shorter slippage length may introduce more spikes in the radiation power profile for a shorter radiation wavelength.

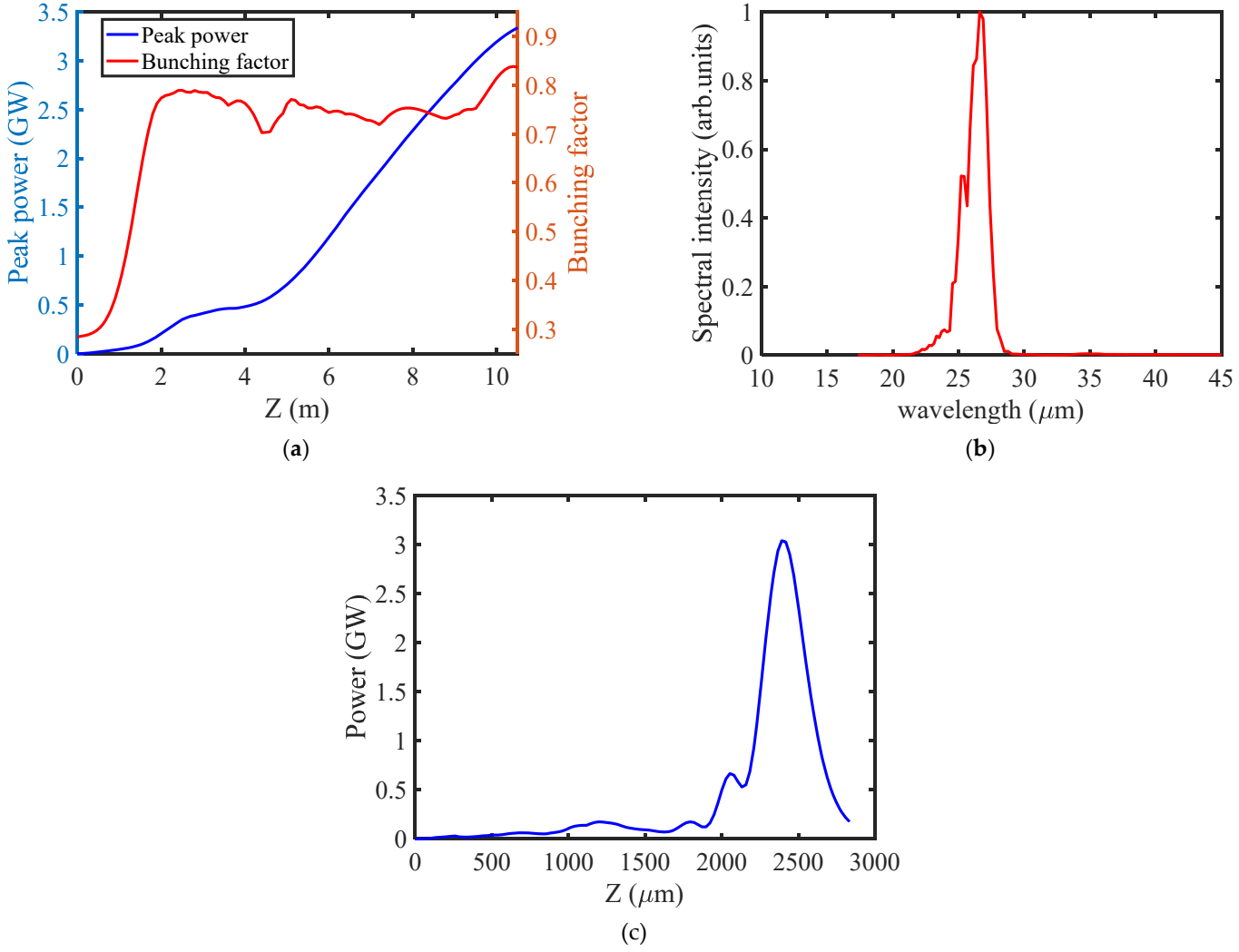

Figure 7. (**a**) The evolutions of power and bunching factor at 11.5 THz along the undulator; (**b**) the final spectrum at 11.5 THz; (**c**) the final power profile at 11.5 THz.

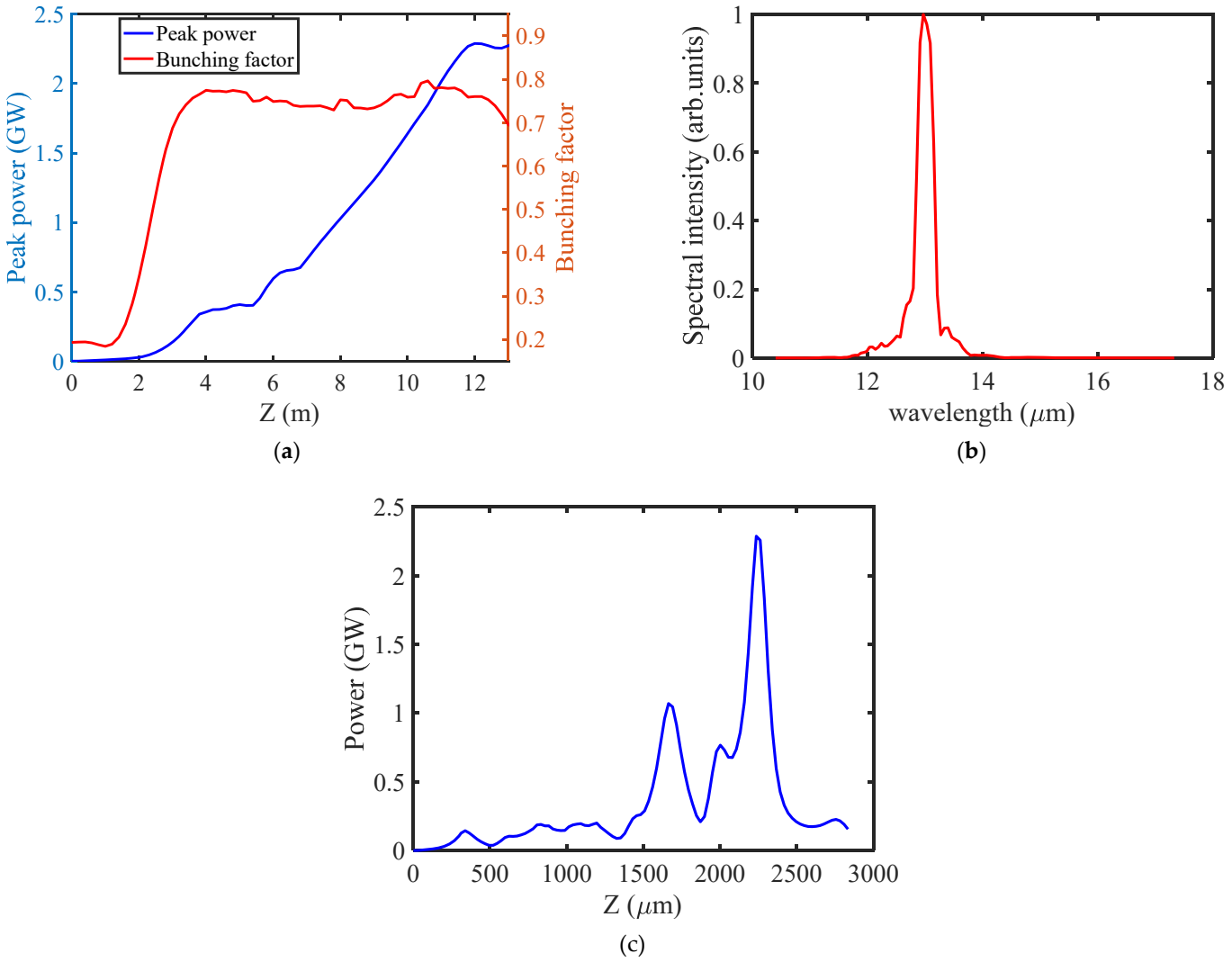

Figure 8. (**a**) The evolutions of power and bunching factor at 23 THz along the undulator; (**b**) the final spectrum at 23 THz; (**c**) the final power profile at 23 THz.

3.3. Performance of the THz Radiation with Undulator at 30 THz and 60 THz

To demonstrate the possible upper limit of the method, simulations of THz radiations at the 30 THz and 60 THz are also performed. Laser parameters introduced in Section 2 are adopted to obtain a laser pulse with a beating frequency of 30 THz. Similarly, the electron beam and the frequency beating laser pulse are sequentially sent into modulator and dispersion sections to imprint bunching into the beam. The phase space and current profile at the exit of chicane are shown in Figure 9. The bunched beam is then sent into undulators to amplify the fundamental (30 THz) and second harmonic (60 THz) of beating frequency signal. The simulation results are shown in Figure 10, where one can find the peak power can also arrive GW-level for radiation at 30 THz and 60 THz. The pulse energy can be calculated as 2.15 mJ for radiation at 30 THz and 1.6 mJ for radiation at 60 THz.

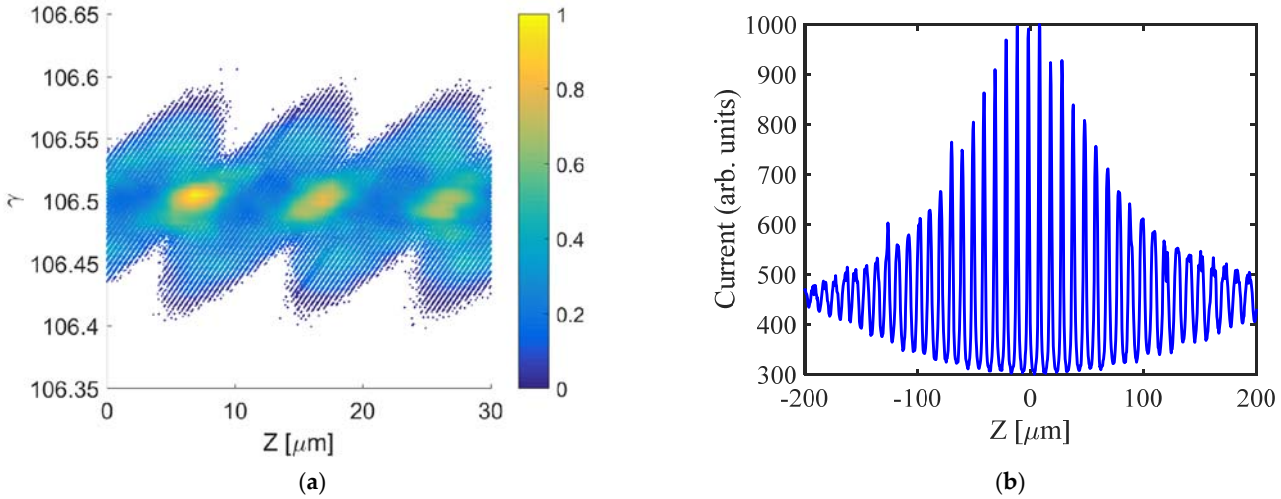

Figure 9. (**a**) The phase space after the dispersion section; (**b**) the current profile after the dispersion section.

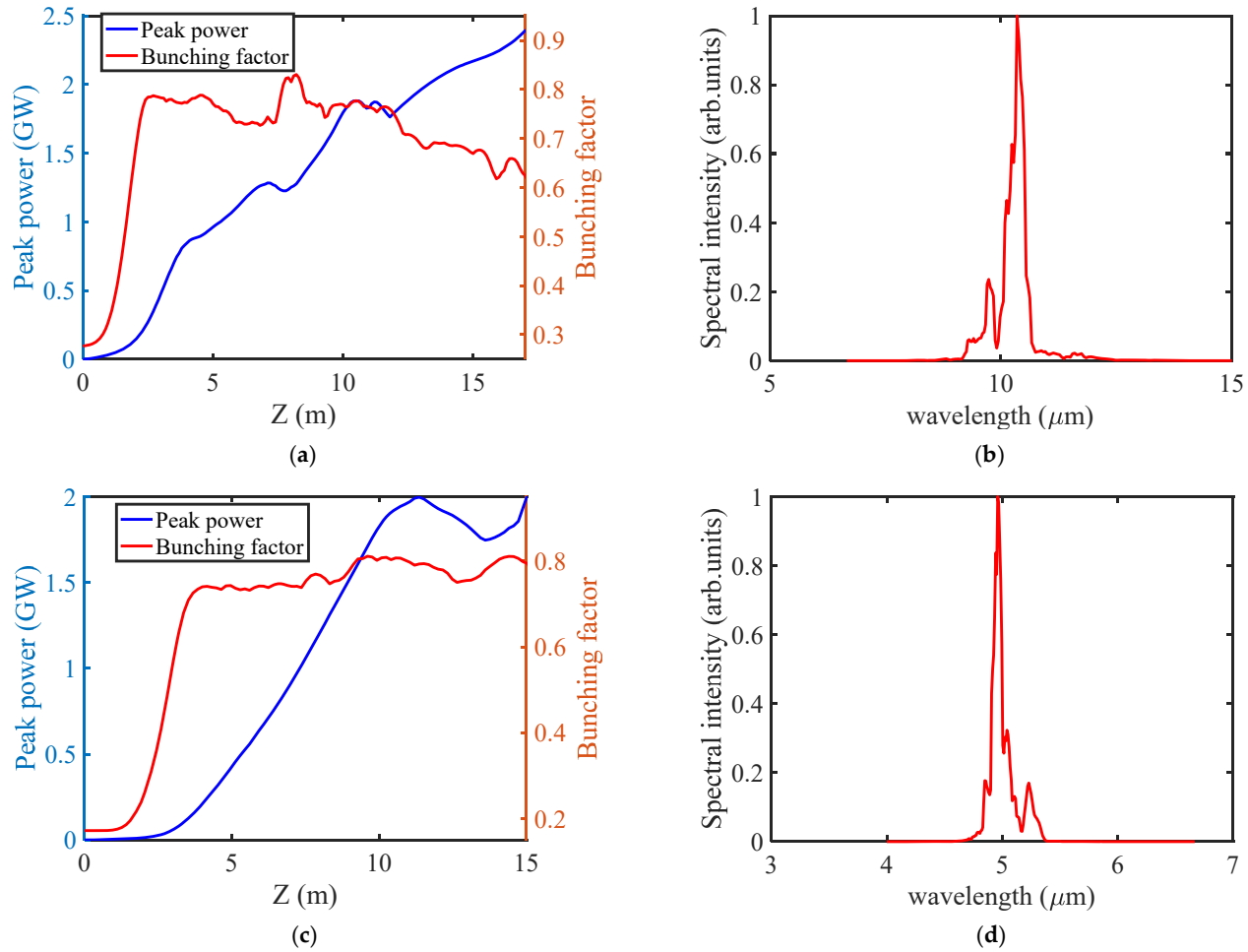

Figure 10. (**a**) The evolutions of power and bunching factor at 30 THz along the undulator; (**b**) the final spectrum at 30 THz; (**c**) the evolutions of power and bunching factor at 60 THz along the undulator; (**d**) the final spectrum at 60 THz.

3.4. Performance with Three Dimensional Effects

In the proposed technique, the beam passes through a magnetic chicane that may introduce CSR, incoherent synchrotron radiation (ISR) and transverse emittance growth. To study these effects, simulations are carried out by combined use of the codes of ELE-

GANT [54] and GENESIS. GENESIS is utilized to perform the simulations in undulators, including the energy modulation and radiation processes, while the density modulation simulation is performed by the ELEGANT, considering the CSR, ISR, and longitudinal space charge effects. The length of each dipole is 1 m, the drift section between the first two dipoles is 3 m and the distance between the middle two dipoles is 0.5 m. As an example, we consider the case of THz radiation at 11.5 THz with a larger R56 of 11 mm, the corresponding bending angle is about 2.8 degree. Figure 11 shows the phase space and current profile at the exit of chicane, where one can find that the density modulation can be well preserved. Similarly, the bunched beam is sent into the undulator to generate intense THz radiation. The peak power and bunching factor evolutions along the undulator and the final spectrum are presented in Figure 11c,d, respectively. The final peak power with three-dimensional effects is lower than that without three-dimensional effects, which is due to the CSR-induced relative energy difference.

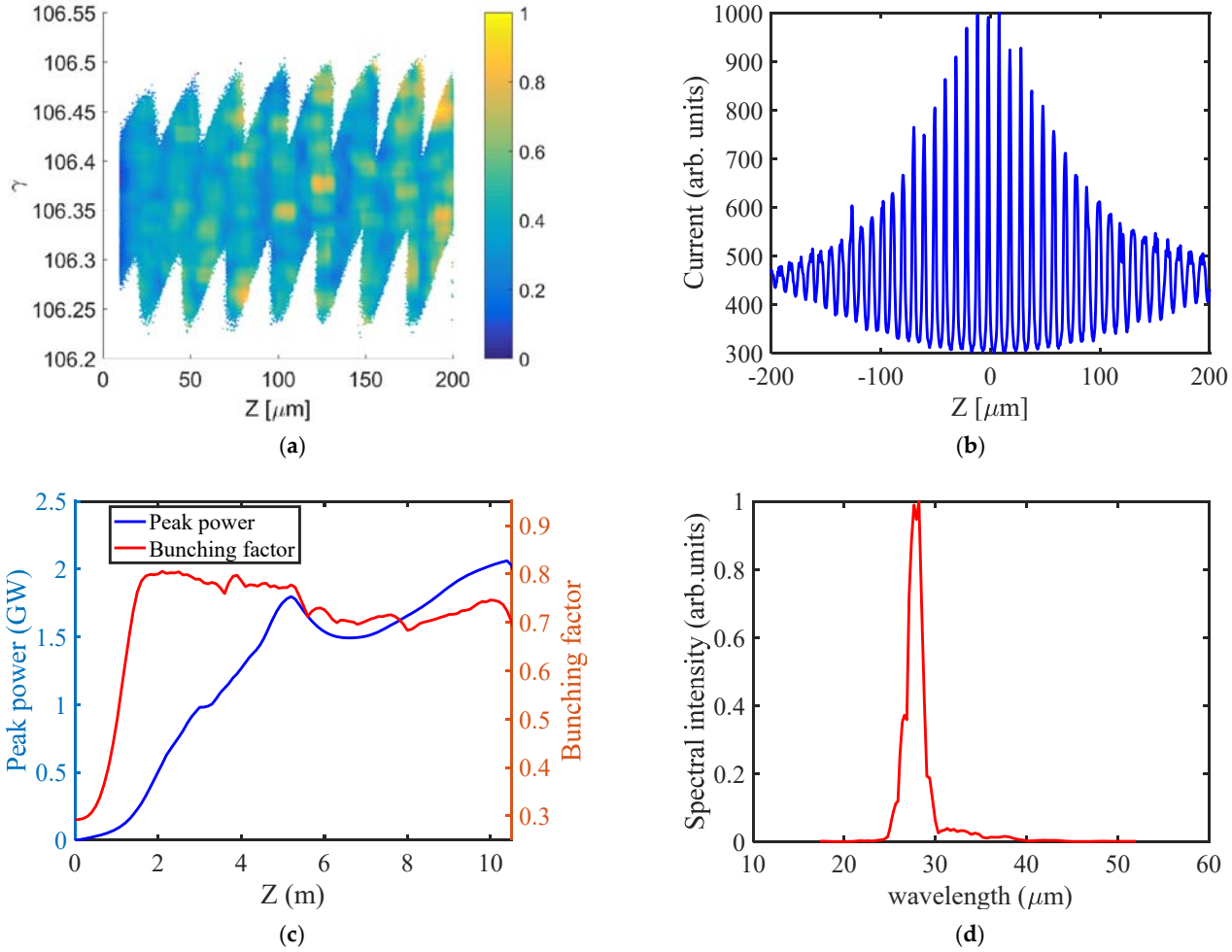

Figure 11. (**a**) The longitudinal phase space after the dispersion section; (**b**) the current profile after the dispersion section; (**c**) the peak power and bunching factor evolutions along the undulator; (**d**) the final spectrum.

4. Discussion and Conclusions

In this paper, a compact accelerator-based light source is proposed to generate THz coherent radiation at mJ level with tunable frequency from 0.1 THz to 60 THz. By using a frequency beating laser modulated electron beam, coherent THz radiation is produced through undulators. Start-to-end simulations are performed, the results show that the proposed technique can produce 11.5 THz and 23 THz coherent radiations with pulse energies of 6.3 mJ and 5 mJ by amplifying the fundamental and second harmonic of the

frequency beating signal. Simulations of THz radiation at the 30 THz and 60 THz are also performed, the results indicate that the pulse energy of THz radiation at 30 THz and 60 THz is 2.15 mJ and 1.6 mJ, respectively. In the proposed technique, the radiation frequency can be continually tuned by tuning the parameters of the seed laser, the electron beam energy, and the undulator gap. It should be noted that the bunched electron beam can also be used to generate THz radiation with other methods, such as coherent synchrotron radiation (CSR) and coherent optical transition radiation (COTR).

In the proposed scheme, the laser power is tuned to satisfy the modulation requirement at certain frequency. A lower THz frequency requires less time delay as well as less laser power. While a larger time delay and a higher peak power are required for a higher THz frequency. To obtain a beating frequency from 0.1 THz to 30 THz, the maximum peak power of laser pulse is about 2 GW, which can be easily achieved by a commercial laser. thus, the pulse energy depends on the pulse length of final THz radiation, which is related to the radiation wavelength. According to the simulation results, the pulse energy of THz radiation at 60 THz is also at the mJ level. According to Equation (4), the generation of high frequency THz radiation requires large linear chirp rate and large time delay. Due to the effects of high-order chirps, the linear chirp may not be well maintained for a large time delay, results in a degradation of the output temporal coherence. To compensate these high order chirps, dispersion elements, such as chirp mirrors, should be adopted in the optical system. In addition, the large time delay can be avoided by increasing the linear chirp rate by using an initially shorter laser pulse. For example, if an initial laser pulse with a pulse length of 11 fs was utilized [55], the required time delay can be reduced to 850 fs for the generation of 30 THz beating frequency. The time delay is just 2.8 times of the stretched pulse length (RMS), and the linear chirp can be well maintained in this region.

The proposed technique is feasible to generate coherent THz radiation with tunable frequency and pulse energy to satisfy various requirements of different scientific frontiers, especially for these require THz pulses with ultra-high pulse energy, such as THz pump-probe, THz triggered chemistry, and single-shot THz bioimaging. In addition, one can consider elliptically polarized undulator (EPU) to generate polarized THz radiation to satisfy various FEL user's requirements. Therefore, the proposed technique may open a new chapter to THz related scientific researches in biology, chemistry, material science, and so on.

Author Contributions: Conceptualization, C.F. and K.Z.; methodology, K.Z. and C.F.; software, K.Z., T.L. and Z.W.; validation, K.Z., Y.K., T.L. and C.F.; formal analysis, K.Z., Y.K. and Z.W.; investigation, K.Z.; data curation, K.Z.; writing—original draft preparation, K.Z.; writing—review and editing, K.Z., C.F. and Y.K.; visualization, K.Z.; supervision, C.F., W.F. and Z.Z.; project administration, C.F., W.F. and Z.Z.; funding acquisition, Z.W., C.F. and K.Z. All authors have read and agreed to the published version of the manuscript.

Funding: This research was funded by National Key Research and Development Program of China, National Natural Science Foundation of China and Shanghai Municipal Science and Technology Major Project, grant number 2018YFE0103100, 11775294, 11905275, 11905277, 12105347, 11975300, 12125508 and 2017SHZDZX02.

Institutional Review Board Statement: Not applicable.

Informed Consent Statement: Not applicable.

Data Availability Statement: Data sharing is not applicable to this article.

Acknowledgments: The authors would like to thank Xiaohao Dong, Bin Li, Zheng Qi, and Li Zeng for helpful discussions and useful comments.

Conflicts of Interest: The authors declare no conflict of interest.

References

1. Tonouchi, M. Cutting-edge terahertz technology. *Nat. Photonics* **2007**, *1*, 97–105. [CrossRef]
2. Shen, Y.; Watanabe, T.; Arena, A.; Kao, C.-C.; Murphy, J.B.; Tsang, T.Y.; Wang, X.J.; Carr, G.L. Nonlinear Cross-Phase Modulation with Intense Single-Cycle Terahertz Pulses. *Phys. Rev. Lett.* **2007**, *99*, 043901. [CrossRef] [PubMed]
3. Gaal, P.; Kuehn, W.; Reimann, K.; Woerner, M.; Elsaesser, T.; Hey, R. Internal motions of a quasiparticle governing its ultrafast nonlinear response. *Nature* **2007**, *450*, 1210–1213. [CrossRef] [PubMed]
4. LaRue, J.; Katayama, T.; Lindenberg, A.; Fisher, A.S.; Öström, H.; Nilsson, A.; Ogasawara, H. THz-Pulse-Induced Selective Catalytic CO Oxidation on Ru. *Phys. Rev. Lett.* **2015**, *115*, 036103. [CrossRef] [PubMed]
5. Mittleman, D.M. Twenty years of terahertz imaging [Invited]. *Opt. Express* **2018**, *26*, 9417–9431. [CrossRef]
6. Kovács, K.; Balogh, E.; Hebling, J.; Tosa, V.; Varjú, K. Quasi-Phase-Matching High-Harmonic Radiation Using Chirped THz Pulses. *Phys. Rev. Lett.* **2012**, *108*, 193903. [CrossRef]
7. Stojanovic, N.; Drescher, M. Accelerator- and laser-based sources of high-field terahertz pulses. *J. Phys. B At. Mol. Opt. Phys.* **2013**, *46*, 192001. [CrossRef]
8. Fülöp, J.A.; Ollmann, Z.; Lombosi, C.; Skrobol, C.; Klingebiel, S.; Pálfalvi, L.; Krausz, F.; Karsch, S.; Hebling, J. Efficient generation of THz pulses with 04 mJ energy. *Opt. Express* **2014**, *22*, 20155–20163. [CrossRef] [PubMed]
9. Vicario, C.; Ovchinnikov, A.V.; Ashitkov, S.I.; Agranat, M.B.; Fortov, V.E.; Hauri, C.P. Generation of 0.9-mJ THz pulses in DSTMS pumped by a Cr:Mg_2SiO_4 laser. *Opt. Lett.* **2014**, *39*, 6632–6635. [CrossRef]
10. Shalaby, M.; Hauri, C.P. Demonstration of a low-frequency three-dimensional terahertz bullet with extreme brightness. *Nat. Commun.* **2015**, *6*, 5976. [CrossRef]
11. Vicario, C.; Monoszlai, B.; Hauri, C.P. GV/mSingle-Cycle Terahertz Fields from a Laser-Driven Large-Size Partitioned Organic Crystal. *Phys. Rev. Lett.* **2014**, *112*, 213901. [CrossRef]
12. Leemans, W.P.; Geddes, C.G.R.; Faure, J.; Tóth, C.; van Tilborg, J.; Schroeder, C.B.; Esarey, E.; Fubiani, G.; Auerbach, D.; Marcelis, B.; et al. Observation of Terahertz Emission from a Laser-Plasma Accelerated Electron Bunch Crossing a Plasma-Vacuum Boundary. *Phys. Rev. Lett.* **2003**, *91*, 074802. [CrossRef] [PubMed]
13. Clerici, M.; Peccianti, M.; Schmidt, B.E.; Caspani, L.; Shalaby, M.; Giguère, M.; Lotti, A.; Couairon, A.; Légaré, F.; Ozaki, T.; et al. Wavelength Scaling of Terahertz Generation by Gas Ionization. *Phys. Rev. Lett.* **2013**, *110*, 253901. [CrossRef]
14. Kim, K.-Y.; Taylor, A.J.; Glownia, J.H.; Rodriguez, G. Coherent control of terahertz supercontinuum generation in ultrafast laser–gas interactions. *Nat. Photonics* **2008**, *2*, 605–609. [CrossRef]
15. Gopal, A.; Herzer, S.; Schmidt, A.; Singh, P.; Reinhard, A.; Ziegler, W.; Brömmel, D.; Karmakar, A.; Gibbon, P.; Dillner, U.; et al. Observation of Gigawatt-Class THz Pulses from a Compact Laser-Driven Particle Accelerator. *Phys. Rev. Lett.* **2013**, *111*, 074802. [CrossRef] [PubMed]
16. Liao, G.-Q.; Li, Y.-T.; Zhang, Y.-H.; Liu, H.; Ge, X.-L.; Yang, S.; Wei, W.-Q.; Yuan, X.-H.; Deng, Y.-Q.; Zhu, B.-J.; et al. Demonstration of Coherent Terahertz Transition Radiation from Relativistic Laser-Solid Interactions. *Phys. Rev. Lett.* **2016**, *116*, 205003. [CrossRef]
17. Liao, G.; Li, Y.; Liu, H.; Scott, G.G.; Neely, D.; Zhang, Y.; Zhu, B.; Zhang, Z.; Armstrong, C.D.; Zemaityte, E.; et al. Multimillijoule coherent terahertz bursts from picosecond laser-irradiated metal foils. *Proc. Natl. Acad. Sci. USA* **2019**, *116*, 3994–3999. [CrossRef] [PubMed]
18. Abo-Bakr, M.; Feikes, J.; Holldack, K.; Wüstefeld, G. Steady-State Far-Infrared Coherent Synchrotron Radiation detected at BESSY II. *Phys. Rev. Lett.* **2002**, *88*, 254801. [CrossRef]
19. Byrd, J.M.; Leemans, W.P.; Loftsdottir, A.; Marcelis, B.; Martin, M.C.; McKinney, W.R.; Sannibale, F.; Scarvie, T.; Steier, C. Observation of Broadband Self-Amplified Spontaneous Coherent Terahertz Synchrotron Radiation in a Storage Ring. *Phys. Rev. Lett.* **2002**, *89*, 224801. [CrossRef]
20. Bielawski, S.; Evain, C.; Hara, T.; Hosaka, M.; Katoh, M.; Kimura, S.; Mochihashi, A.; Shimada, M.; Szwaj, C.; Takahashi, T.; et al. Tunable Narrowband Terahertz Emission from Mastered Laser–Electron Beam Interaction. *Nat. Phys.* **2008**, *4*, 390–393. [CrossRef]
21. Zhang, Z.; Fisher, A.S.; Hoffmann, M.C.; Jacobson, B.; Kirchmann, P.S.; Lee, W.-S.; Lindenberg, A.; Marinelli, A.; Nanni, E.; Schoenlein, R.; et al. A High-Power, High-Repetition-Rate THz Source for Pump–Probe Experiments at Linac Coherent Light Source II. *J. Synchrotron Radiat.* **2020**, *27*, 890–901. [CrossRef]
22. Di Mitri, S.; Perucchi, A.; Adhlakha, N.; Di Pietro, P.; Nicastro, S.; Roussel, E.; Spampinati, S.; Veronese, M.; Allaria, E.; Badano, L.; et al. Coherent THz Emission Enhanced by Coherent Synchrotron Radiation Wakefield. *Sci. Rep.* **2018**, *8*, 11661. [CrossRef]
23. Yang, X.; Brunetti, E.; Gil, D.R.; Welsh, G.; Li, F.; Cipiccia, S.; Ersfeld, B.; Grant, D.W.; Grant, P.A.; Islam, M.R.; et al. Three Electron Beams from a Laser-Plasma Wakefield Accelerator and the Energy Apportioning Question. *Sci. Rep.* **2017**, *7*, 43910. [CrossRef] [PubMed]
24. Wu, Z.; Fisher, A.S.; Goodfellow, J.; Fuchs, M.; Daranciang, D.; Hogan, M.; Loos, H.; Lindenberg, A. Intense terahertz pulses from SLAC electron beams using coherent transition radiation. *Rev. Sci. Instruments* **2013**, *84*, 022701. [CrossRef] [PubMed]
25. Daranciang, D.; Goodfellow, J.; Fuchs, M.; Wen, H.; Ghimire, S.; Reis, D.A.; Loos, H.; Fisher, A.S.; Lindenberg, A.M. Single-Cycle Terahertz Pulses with >0.2 V/Å Field Amplitudes via Coherent Transition Radiation. *Appl. Phys. Lett.* **2011**, *99*, 141117. [CrossRef]
26. Green, B.; Kovalev, S.; Asgekar, V.; Geloni, G.; Lehnert, U.; Golz, T.; Kuntzsch, M.; Bauer, C.; Hauser, J.; Voigtlaender, J.; et al. High-Field High-Repetition-Rate Sources for the Coherent THz Control of Matter. *Sci. Rep.* **2016**, *6*, 22256. [CrossRef] [PubMed]
27. Tanaka, T. Difference frequency generation in free electron lasers. *Opt. Lett.* **2018**, *43*, 4485–4488. [CrossRef] [PubMed]

28. Tanikawa, T.; Karabekyan, S.; Kovalev, S.; Casalbuoni, S.; Asgekar, V.; Serkez, S.; Geloni, G.; Gensch, M. A superradiant THz undulator source for XFELs. *J. Instrum.* **2019**, *14*, P05024. [CrossRef]
29. Liang, L.; Liu, W.; Jia, Q.; Wang, L.; Lu, Y. High-harmonic terahertz Smith-Purcell free-electron-laser with two tandem cylindrical-gratings. *Opt. Express* **2017**, *25*, 2960–2968. [CrossRef]
30. Bonifacio, R.; Pellegrini, C.; Narducci, L. Collective instabilities and high-gain regime in a free electron laser. *Opt. Commun.* **1984**, *50*, 373–378. [CrossRef]
31. Andruszkow, J.; Aune, B.; Ayvazyan, V.; Baboi, N.; Bakker, R.; Balakin, V.; Barni, D.; Bazhan, A.; Bernard, M.; Bosotti, A.; et al. First Observation of Self-Amplified Spontaneous Emission in a Free-Electron Laser at 109 nm Wavelength. *Phys. Rev. Lett.* **2000**, *85*, 3825–3829. [CrossRef] [PubMed]
32. Huang, Z.; Kim, K.-J. Review of x-ray free-electron laser theory. *Phys. Rev. Spéc. Top. Accel. Beams* **2007**, *10*, 034801. [CrossRef]
33. Tiedtke, K.; Azima, A.; Von Bargen, N.; Bittner, L.; Bonfigt, S.; Düsterer, S.; Faatz, B.; Frühling, U.; Gensch, M.; Gerth, C.; et al. The soft x-ray free-electron laser FLASH at DESY: Beamlines, diagnostics and end-stations. *N. J. Phys.* **2009**, *11*, 023029. [CrossRef]
34. Li, Y.; Kim, K.-J. Nonrelativistic electron bunch train for coherently enhanced terahertz radiation sources. *Appl. Phys. Lett.* **2008**, *92*, 014101. [CrossRef]
35. Shen, Y.; Yang, X.; Carr, G.L.; Hidaka, Y.; Murphy, J.B.; Wang, X. Tunable Few-Cycle and Multicycle Coherent Terahertz Radiation from Relativistic Electrons. *Phys. Rev. Lett.* **2011**, *107*, 204801. [CrossRef]
36. Liu, W.; Lu, Y.; He, Z.; Li, W.; Wang, L.; Jia, Q. Broad-tunable terahertz source with over-mode waveguide driven by train of electron bunches. *Opt. Express* **2016**, *24*, 4109–4116. [CrossRef] [PubMed]
37. Muggli, P.; Yakimenko, V.; Babzien, M.; Kallos, E.; Kusche, K.P. Generation of Trains of Electron Microbunches with Adjustable Subpicosecond Spacing. *Phys. Rev. Lett.* **2008**, *101*, 054801. [CrossRef]
38. Sun, Y.-E.; Piot, P.; Johnson, A.; Lumpkin, A.H.; Maxwell, T.J.; Ruan, J.; Thurman-Keup, R. Tunable Subpicosecond Electron-Bunch-Train Generation Using a Transverse-To-Longitudinal Phase-Space Exchange Technique. *Phys. Rev. Lett.* **2010**, *105*, 234801. [CrossRef] [PubMed]
39. Zhang, Z.; Yan, L.; Du, Y.; Zhou, Z.; Su, X.; Zheng, L.; Wang, D.; Tian, Q.; Wang, W.; Shi, J.; et al. Tunable High-Intensity Electron Bunch Train Production Based on Nonlinear Longitudinal Space Charge Oscillation. *Phys. Rev. Lett.* **2016**, *116*, 184801. [CrossRef]
40. Antipov, S.; Babzien, M.; Jing, C.; Fedurin, M.; Gai, W.; Kanareykin, A.; Kusche, K.; Yakimenko, V.; Zholents, A. Subpicosecond Bunch Train Production for a Tunable mJ Level THz Source. *Phys. Rev. Lett.* **2013**, *111*, 134802. [CrossRef] [PubMed]
41. Xiang, D.; Stupakov, G. Enhanced tunable narrow-band THz emission from laser-modulated electron beams. *Phys. Rev. Spéc. Top. Accel. Beams* **2009**, *12*, 080701. [CrossRef]
42. Dunning, M.; Hast, C.; Hemsing, E.; Jobe, K.; McCormick, D.; Nelson, J.; Raubenheimer, T.O.; Soong, K.; Szalata, Z.; Walz, D.; et al. Generating periodic terahertz structures in a relativistic electron beam through frequency down-conversion of optical lasers. *Phys. Rev. Lett.* **2012**, *109*, 074801. [CrossRef] [PubMed]
43. Zhang, Z.; Yan, L.; Du, Y.; Huang, W.; Tang, C.; Huang, Z. Generation of high-power, tunable terahertz radiation from laser interaction with a relativistic electron beam. *Phys. Rev. Accel. Beams* **2017**, *20*, 050701. [CrossRef]
44. Zhang, H.; Wang, W.; Jiang, S.; Li, C.; He, Z.; Zhang, S.; Jia, Q.; Wang, L.; He, D. Tuning electron bunch with a longitudinally shaped laser to generate half-cycle terahertz radiation pulse. *J. Instrum.* **2021**, *16*, P08019. [CrossRef]
45. Kan, K.; Huang, Z.; Marcus, G.; Zhang, Z. Intense THz source based on laser modulator and bunch compressor with electron beam ranging from 35 to 50 MeV. *Nonlinear Dyn. Collect. Eff. Part. Beam Phys.* **2019**, 285–297. [CrossRef]
46. Aniruddha, S.; Weling, S.; Auston, D.H. Novel sources and detectors for coherent tunable narrow-band terahertz radiation in free space. *J. Opt. Soc. Am.* **1996**, *13*, 2783–2791.
47. Xiang, D.; Stupakov, G. Echo-enabled harmonic generation free electron laser. *Phys. Rev. Spéc. Top. Accel. Beams* **2009**, *12*, 030702. [CrossRef]
48. Wigner, E. On the Quantum Correction for Thermodynamic Equilibrium. *Phys. Rev.* **1932**, *40*, 749–759. [CrossRef]
49. Gase, R. The Wigner distribution function applied to laser radiation. *Opt. Quantum Electron.* **1992**, *24*, S1109–S1118. [CrossRef]
50. Available online: http://tesla.desy.de/~{}meykopff/ (accessed on 13 December 2021).
51. Zeng, L.; Feng, C.; Wang, X.; Zhang, K.; Qi, Z.; Zhao, Z. A Super-Fast Free-Electron Laser Simulation Code for Online Optimization. *Photonics* **2020**, *7*, 117. [CrossRef]
52. Reiche, S. GENESIS 1.3: A fully 3D time-dependent FEL simulation code. *Nucl. Instrum. Methods Phys. Res. Sect. A Accel. Spectrometers, Detect. Assoc. Equip.* **1999**, *429*, 243–248. [CrossRef]
53. Ferrario, M.; Alesini, D.; Bacci, A.; Bellaveglia, M.; Boni, R.; Boscolo, M.; Castellano, M.; Chiadroni, E.; Cianchi, A.; Cultrera, L.; et al. Experimental Demonstration of Emittance Compensation with Velocity Bunching. *Phys. Rev. Lett.* **2010**, *104*, 054801. [CrossRef] [PubMed]
54. Borland, M. *Elegant: A flexible SDDS-Compliant Code for Accelerator Simulation*; Argonne National Lab: Lemont, IL, USA, 2000.
55. Zhou, X.; Lee, H.; Kanai, T.; Adachi, S.; Watanabe, S. An 11-fs, 5-kHz optical parametric/Ti:sapphire hybrid chirped pulse amplification system. *Appl. Phys. B.* **2007**, *89*, 559–563. [CrossRef]